



Force signal alignment in dynamic testing machine calibration applications[☆]

Miha Hiti 

Slovenian Building and Civil Engineering Institute (ZAG), Ljubljana, Slovenia

ARTICLE INFO

Keywords:

Force
Calibration
Dynamic systems
Time-synchronisation
Cross-correlation

ABSTRACT

Calibration of force in measuring systems where the force is time dependent i.e. dynamically changing, introduces additional complexities versus quasi-static calibration conditions. Time variable force signals necessitate accurate time alignment between concurrent signals – measurement series from unit under test and the measurement series from the reference standard need to be synchronised. Different unsynchronised measuring systems are typically used for acquisition of each calibration signal and they need to be time aligned in post-processing to eliminate as much as possible the influence of the sample misalignment from the resulting testing machine indication error. The paper focuses on the time synchronization of measurement series by using cross-correlation to determine the necessary time correction when calibrating testing machines with dynamic cyclic force excitation. Measurements are presented for calibration signals in the examples of 20 kN testing machine compression calibration for $5 \text{ kN} \pm 1 \text{ kN}$ cycling force with 1 Hz, 5 Hz, and 10 Hz cycling frequencies, and 1000 kN testing machine tensile calibration for $500 \text{ kN} \pm 100 \text{ kN}$ cycling force with 1 Hz cycling frequency. The standard deviation of the error distribution after time correction and clock rate compensation was below 0.2 % for both, 20 kN testing machine calibration, and 1000 kN testing machine calibration.

1. Introduction

Industrial and research applications of force measurements are by nature generally dynamic, where the force is not constant during the measurement process, but is changing either rapidly or slowly with time. When such force measuring systems require calibration to assure metrological traceability, mostly only static or quasi-static procedures are available, based on measurements during constant force conditions. Most international standards, that currently exist for calibration of force measuring instruments, require loading profiles with clearly defined force steps to keep the force stable when the values are acquired – such as the ISO 376 [1] standard for calibration of force-proving instruments (transfer standards) used for the verification of uniaxial testing machines. Also the application of these force-proving instruments to transfer the force traceability to material testing machines follows typically a similar stepwise loading profile, such as, for example, the procedure defined in the international standard ISO 7500-1 [2] for calibration and verification of static uniaxial testing machines. The latter also allows as an option a calibration procedure where the force is slowly continuously increasing and decreasing, but, as previous research

has shown, the slow continuous force application instead of the loading in force steps already leads to significant calibration errors if no additional precautions are taken for the calculation of the calibration results [3–5]. What seems as an excessive calibration error in these cases is in reality usually not the problem of the indication error of the testing machine, but the result of inappropriate error analysis and calculation, where the measured values from the reference system and the testing machine did not correspond to the same moment in time [6]. Such measurement signal delays or time misalignments can occur even within the same measurement system where multiple channels are nominally synchronised [7] and become only more problematic when comparing signals from two independent measurement systems [8].

In general, any measurement system where the quantity depends on time, e.g. the force changes dynamically, the additional effects increase the complexity of the evaluation in contrast to the usual conditions of quasi-static or static calibration. The fundamental requirement in the case of time variable force signals evaluation is that the measurements from the unit under test and the measurements from the reference standard are synchronised first. These measurements are largely acquired by separate measuring systems, which are inherently not

[☆] This article is part of a special issue entitled: ‘MEASUR_XXIV IMEKO World Congress’ published in Measurement.

E-mail address: miha.hiti@zag.si.

synchronised, and in most cases time-uncalibrated – the clock rates of the measurement system are not calibrated, neither in terms of absolute time nor are they calibrated in terms of relative time or time intervals. Since it is difficult, and sometimes not possible, to synchronise the measurement instrumentation during the data acquisition, synchronisation must be done in post processing by aligning the reference signals and the testing machine signals according to a common time base. In any case, it needs to be assured that the acquired signals correspond to the actual measured signals so it is mandatory to acquire the data streams of dynamic signals continuously with an appropriate (high enough) sampling frequency and appropriate filter settings to prevent signal aliasing.

However, even if above precautions are taken to acquire the signals correctly and as synchronously as possible, different effects such as filter settings, difference in the sampling frequency, data processing delay and unsynchronised measurement starts can introduce a time misalignment between the measured signal sequences even for basically identical signals making the comparison difficult. Without the synchronisation of the signals, the comparison errors are arbitrary and can make calibration errors appear to be anywhere between 0 % and more than 100 % of the applied amplitude. The resulting error from such measurements is in no way linked to the actual testing machine indication error and cannot be used for any meaningful evaluation. Removing or reducing the error due to the time misalignment is key in determining the actual error in the force indication.

The paper focuses on the time alignment of measurement sequences at testing machine calibration where the force is dynamically cycled. The measurements were made in the scope of the Joint Research Project within the European Metrology Research Programme EMPIR 18SIB08 ComTraForce, dealing with methods, instrumentation, and guidelines for extension of static force traceability to continuous and dynamic force calibration from NMI level to industry level applications [9]. Within the project, several guidelines were prepared addressing the issues of dynamic testing machine calibration. One of the project outcomes resulted in a German DKD guideline DKD-R 9-4 [10]. The guideline proposes a procedure for the calibration of testing machines with cyclic excitation, the data acquisition requirements regarding sampling rate and filter settings, and data stream evaluation. During calibration, the machine is expected to stabilise the cycling before data acquisition and include within the acquired data stream a characteristic disturbance, in a form of amplitude change, to allow for easier data synchronisation of the signals in post-processing. The guideline recommends for cyclic sinusoidal excitation a sampling rate of at least 80 samples per cycle, and no low-pass filter or low-pass filter set at about 10 %–15 % of the sampling frequency. Minimum and maximum amplitude cycle values and peak-to-peak amplitudes from the machine and the calibration system are also to be acquired. Data evaluation is then performed by fitting the data streams, calculating the means, amplitude spans, and phase delays of the fitted and measured signals, and expressing the results of the peak-to-peak and min–max deviation comparison for the cycles, similar to ISO 4965-1 [11]. The full synchronization of the signals is not necessary for such evaluation as the comparison is obtained on cycle-to-cycle characteristics basis instead of on sample-to-sample basis. No synchronization procedure is currently given or recommended in the guideline. In this paper however, the possibility of the direct comparison of the testing machine and the reference calibration system data for the full acquired sequence interval is explored. In this case, the exact signal synchronisation is first necessary to allow sample-to-sample comparison and error calculation for the whole calibration sequence.

2. Methods and procedure

Two testing systems were selected for calibration under dynamic conditions. Both are hydraulically driven material testing machines widely used in industrial and research applications for testing of mechanical properties of materials such as metal, polymer, or wood samples. For performing testing activities, especially for accredited standard

testing methods, the force measuring systems of such testing machines need to be calibrated to assure metrological traceability of the test results. While the static force calibration of these testing machines is straightforward and widely available from various accredited calibration laboratories the dynamically changing force calibration still poses a challenge, not only as the dynamically calibrated force transfer standards are not available but because already the dynamic measurement acquisition and evaluation by itself is more complex than the static measurement acquisition with regard to comparability of acquired measurement results.

The aim of the research was to explore signal alignment techniques of dynamically acquired force signals to cover the typical range of material testing machine applications that are often encountered in testing machine calibration activities. The tests were designed to include a material testing machine in the lower, more widespread, range of 20 kN and a material testing machine with a higher force range of 1000 kN. During investigation, both loading modes were included in the tests, the tensile loading and compressive loading. Furthermore, different real world sampling rates and filter settings were selected for analysis. Typical calibration equipment was employed that would be also used for static calibration of the testing machines. The dynamic force excitation was selected within the machine range, in one loading direction, with no dynamic excitation through zero. Selected dynamic excitation frequencies were in the range from 1 Hz to 10 Hz. The loading procedure was roughly based on recommendations in guideline DKD-R 9-4 for sinusoidal excitation.

2.1. Testing systems

The lower force range dynamic testing machine was a MTS Bionix of 20 kN force capacity, Fig. 1. The testing machine for the dynamic measurements in the higher force range was a ZwickRoell HB 1000 dynamic testing machine of 1000 kN capacity, Fig. 2. Each machine was controlled by its dedicated PC with the manufacturers testing software. The testing machine force data was logged by each PC during calibration procedures and was exported for analysis after the tests.

The reference force measuring equipment for the lower force range consisted of an HBM U10M 25 kN force transducer connected to an HBM MGCplus system with HBM ML55B 4.8 kHz carrier frequency strain-gauge amplifier module. The measurements from the reference system were acquired by HBM Catman software running on a separate PC. The reference transducer was positioned in the machine for compressive axial loading.

The reference force measuring equipment for the higher force range consisted of a GTM ZST 1000 kN force transducer connected to the HBM MGCplus system with HBM ML55B 4.8 kHz carrier frequency strain-gauge amplifier module. The measurements from the reference system were also in this case acquired by HBM Catman software running on a separate PC. The reference transducer was positioned in the machine for tensile axial loading.

The 25 kN HBM U10M force transducer and the 1000 kN GTM ZST force transducers were calibrated statically according to ISO 376 calibration procedures, and the measuring amplifier HBM ML55B was also calibrated under static conditions only.

Both force applications to the reference transducer were following the requirements for mounting parts of the ISO 376 and ISO 7500-1 standard for axial testing machine verification, the compression loading was via a standard loading pad and the tensile calibration via standard ball cups and ball nuts.

2.2. Measurement acquisition

The 20 kN testing machine was set-up to generate first a stable force of 5 kN, loading the reference transducer in compressive mode. Then the force cycling was started around the 5 kN force with a sinusoidal excitation with a defined frequency and amplitude variation of ± 1 kN. In

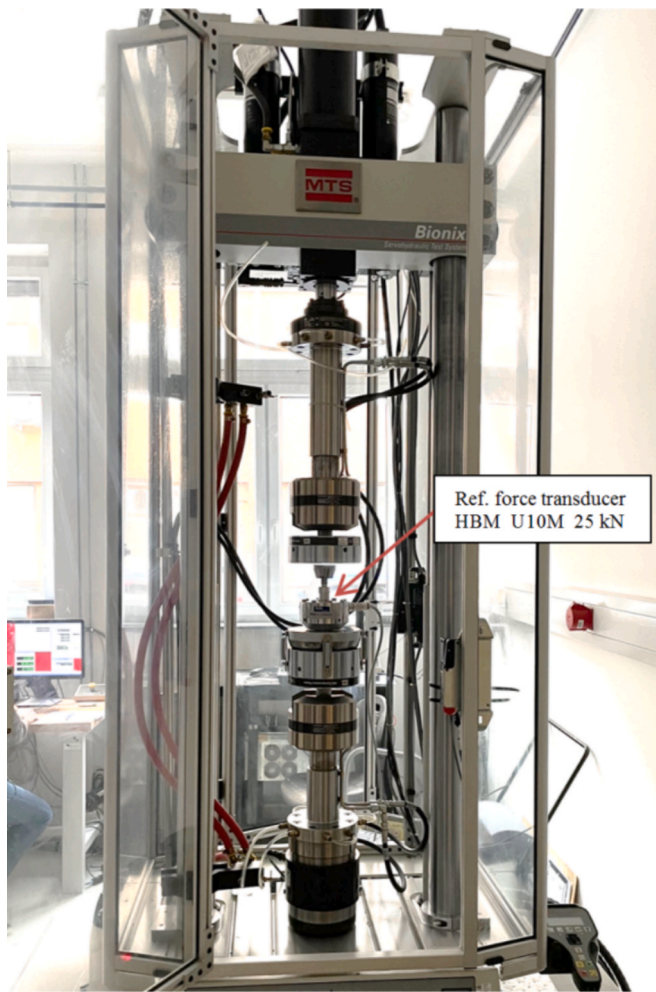


Fig. 1. 20 kN dynamic testing machine MTS Bionix with HBM U10M 25 kN reference force transducer.



Fig. 2. 1000 kN dynamic testing machine ZwickRoell HB 1000 with GTM ZST 1000 kN reference force transducer.

the last part of the sequence, the cycling was stopped to bring the force back to the stable 5 kN value, as shown in Fig. 3 with the blue curve (MTS).

The reference force measuring system consisting of the HBM U10M 25 kN force transducer and the HBM ML55B measuring amplifier was set up with a 1200 Hz sampling rate (nominal). A Butterworth low pass filter with a relatively high value of 1000 Hz was set on the amplifier to limit the effect of the amplifier filter setting as the testing machine filter setting was unknown. This high value of the low-pass filter of the amplifier effectively simulated a measurement without a low-pass filter. The total length of the acquired force data sequence was about 25 s.

The comparison of the signal from the reference force measuring system (red curve – ML55B) to the signal from the force measuring system of the testing machine (blue curve – MTS) is also visible in Fig. 3. The signals are shown in the form as they were acquired with all unwanted effects present. The direct comparison of these signals can only be made at the start of the sequence and at the end of the sequence, where the force is stable in both signals and hovering around 5 kN force value. These parts of the sequence are similar to a static calibration of the testing machine and give a realistic calibration error even though it is evident from both sequences, that there was a significant time delay present during the data acquisition. In the part of the dynamic signal, the error calculation will not be correct as the signals are out of sync due to a number of possible reasons. These can be either arising from different data acquisition systems, the non-synchronized starts of the measurements, the variation in the sampling frequencies, and the differences in

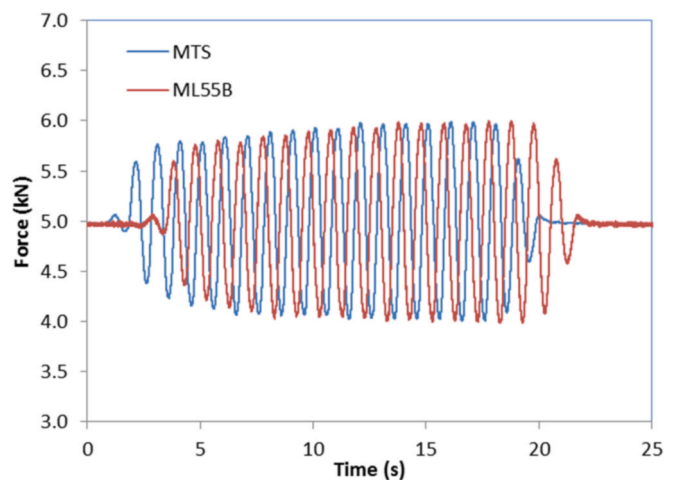


Fig. 3. Direct comparison of force signal sequences from the 20 kN testing machine (MTS) and the reference calibration system (ML55B).

time-bases or clock rates of PCs employed for data acquisition

To investigate the effect of the force excitation frequency, the above procedure was repeated for three excitation frequencies in the range from 1 Hz to 10 Hz, Fig. 4. The selected excitation frequencies were 1 Hz as shown in Fig. 4(a), 5 Hz as shown in Fig. 4(b), and 10 Hz as shown in

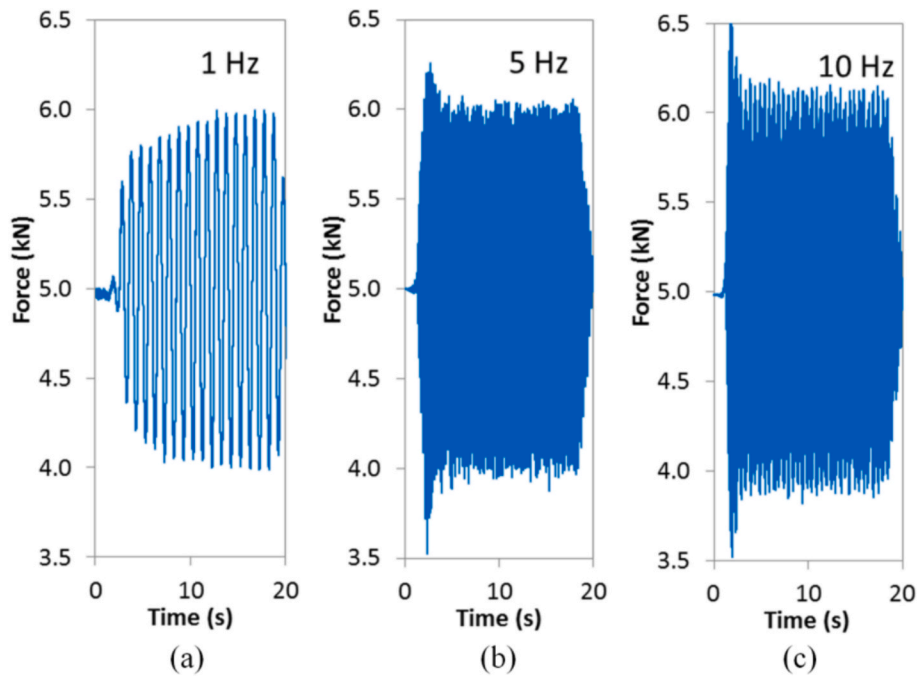


Fig. 4. Cyclic excitation of the reference force transducer in the 20 kN dynamic testing machine with $5 \text{ kN} \pm 1 \text{ kN}$ force for (a) 1 Hz, (b) 5 Hz, and (c) 10 Hz, as measured by the machine's force measuring system.

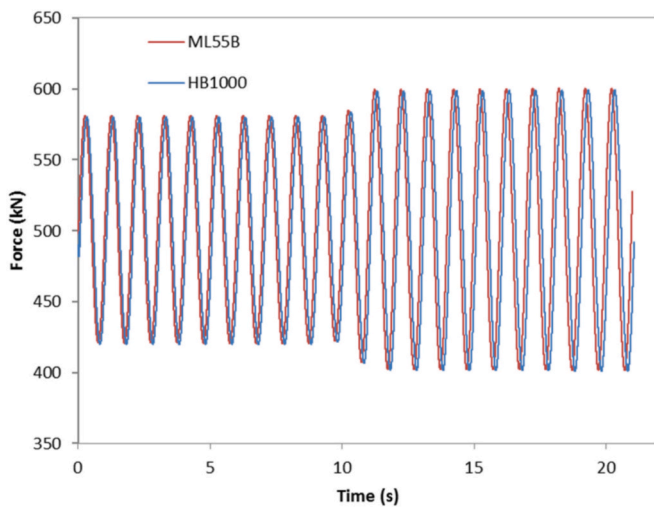


Fig. 5. Comparison of force signal sequences from testing machine (HB1000) and the reference calibration system (ML55B) for cyclic tensile force $500 \text{ kN} \pm 80 \text{ kN}$ and the switch to $500 \text{ kN} \pm 100 \text{ kN}$ (signals approximately aligned visually).

Fig. 4(c). The force measurement data acquisition rate of the machine was set to 1024 Hz (nominal), with an unknown low pass filter setting. The time interval was selected to record the transition from the stable force of 5 kN to cycling with an amplitude of $\pm 1 \text{ kN}$ (between 4 kN and 6 kN) and stabilising at 5 kN again. It can be seen in Fig. 4, that the superimposed excitation resulted in different system responses depending on the frequency of excitation. For the 1 Hz excitation, the amplitude of the oscillation reached the required value only after significant time of slowly approaching the final amplitude value, while for the 5 Hz and 10 Hz excitations the amplitude exhibits an overshoot at the beginning of the oscillation and requires several periods of oscillation to stabilise. In all three cases, it can also be seen, that the amplitude of the oscillation is not stable and varies slightly with time.

The 1000 kN testing machine was set-up to generate a 500 kN tensile force with a sinusoidal amplitude variation first of $\pm 80 \text{ kN}$ (cycling between 420 kN and 580 kN tensile force) and then increased to $\pm 100 \text{ kN}$ (cycling between 400 kN and 600 kN tensile force), shown as the blue curve in Fig. 5 (HB1000). The cycling frequency was set to 1 Hz. The force data acquisition rate of the machine was set to 200 Hz (nominal), with an unknown low pass filter setting.

The reference force measuring system consisting of the GTM ZST 1000 kN force transducer and the HBM ML55B measuring amplifier was set up with a 1200 Hz sampling rate (nominal), and a 100 Hz Butterworth low pass filter was set on the amplifier. The total reference system data acquisition time interval was about 25 s and was started when the force of the testing machine was already oscillating with the amplitude of $\pm 80 \text{ kN}$ for some time. The time interval was selected to record the transition from the cycling amplitude of $\pm 80 \text{ kN}$ to $\pm 100 \text{ kN}$. After the end of the reference system data acquisition interval the machine continued to cycle with the amplitude of $\pm 100 \text{ kN}$.

Also in this case a significant time misalignment is unavoidable due to different data acquisition systems, the unsynchronised measurement starts, the different sampling rates, and the unsynchronised time bases of PCs. The comparison of the acquired data signals from the testing machine's force measuring system and from the reference force measuring system can be seen in Fig. 5, where the signals have been approximately visually aligned in post-processing. The amplitude oscillation change from $\pm 80 \text{ kN}$ to $\pm 100 \text{ kN}$ can be seen after the first 10 s duration of the shown series. With the approximate manual alignment in post-processing for the signals in Fig. 5, the deviation between the signals was in the range of $\pm 5\% - \pm 10\%$.

In both cases of testing machine calibration the reference signal and the machine measurement signal need to be synchronised before the calibration error determination. Failure to properly synchronise the signals can lead to arbitrary error values exceeding the cycling amplitude of the signals. The synchronisation of the signals can in theory be performed at the data acquisition stage or in post-processing. In the case of testing machine calibration, synchronisation at the data acquisition stage, such as hardware acquisition triggering, clock synchronisation, or time calibration is in most cases technically not possible due to the testing machine hardware and software limitations or would require

additional hardware. The post-processing synchronisation approach is in such cases preferable as the procedure typically requires analysing and manipulating the signals after the measurements have been finished to determine phase shift and delays. The easiest method to align the signals in post processing is to find some common distinct reference waveform shapes, such as a spike or an irregularity that are present within both signals and manually correcting the signal sequence to try to achieve a good alignment. In the case of the 20 kN testing machine calibration, this could be the transition from the stable signal to the oscillating force present in both signals and the change of amplitude from ± 80 kN to ± 100 kN in the case of the 1000 kN testing machine calibration. These signal features could be used to try to visually align the signals, but if there is no such common reference, other methods need to be applied [12–14], also giving more objective and robust alignment results.

2.3. Signal alignment procedure

In many engineering and scientific fields a widely used procedure for mathematical time delay determination between two similar signals is the calculation of a discrete cross-correlation function [15]. Many mathematical synchronisation techniques are known [16], but the cross-correlation provides a simple and most straightforward approach. While the discrete cross-correlation analysis can be performed either in the time domain or in the frequency domain, in this paper, the cross-correlation function in the time domain is used to determine the time delay between the two signals (i.e. the phase shift). The evaluation in the frequency domain would be of benefit for large datasets as it produces results faster. The discrete cross-correlation function works by sliding one signal over the other and finding the maximum value for best match according to (1), where R is the discrete cross-correlation function for signals x and y , n is the sample index, N the total number of samples and k the introduced shift between the signal samples.

$$R_{xy}[k] = \sum_{n=k}^{N-1} x[n] \cdot y[n-k] \quad (1)$$

The function has a maximum value where the overlap of the two signals is the best and the number of the samples k for which the signals have been shifted to obtain this maximum value gives the required information about the necessary time shift to align the signals for best fit. From the number of shifted samples and the sampling rate of the sequences the optimal time shift can be estimated and corrected before the testing machine indication error is calculated.

The cross-correlation calculation is only applicable to signals that have the same frequency rate. The reason for this is that during calculation of (1) each sample from the first signal sequence is multiplied with a corresponding sample from the second signal sequence. This is done for each signal sample pair of the sequence. There is no time information in (1), so only samples with the same time interval can be compared. If the interval is not the same in both sequences the calculation will not give correct results.

In cases, where the amplitude of the signals are not equal, normalization of the signals can be performed before cross correlation calculation, by subtracting the mean value from each signal and dividing each signal by its standard deviation. This is especially useful, when comparing low values of raw force transducer output in mV/V and the testing machine indication in the unit of force.

When the sequences are prepared with the same sample interval and normalized if necessary, the evaluation can continue by calculation of the cross-correlation function. The shift, for which the maximum result of the calculation is obtained, then represents the best estimates of the required signal shift where both signal sequences are aligned optimally.

The time shift result is used for the correction of the time delay between the signals, and the machine indication error q is calculated following (2) for each signal sample index n of aligned signal sequences for machine indication y and reference force system x .

$$q[n] = \frac{y[n] - x[n]}{x[n]} \quad (2)$$

The calculated error from (2) includes effects from any remaining misalignment as well as effects from any difference in clock rates from different acquisition systems. In the case of different clock rates, the sampling frequency used to resample the signals is also affected which leads to incorrect sample pairs when performing the cross-correlation calculation. Where the clock rates are not the same, one signal can be linearly scaled in the time axis and the signal sequence resampled to match the other signal's clock rate before applying the cross-correlation function.

Fig. 6 shows an example of the effect of clock rate deviation influence after synchronization with cross-correlation for the signals in Fig. 3. The cross-correlation function suggested the alignment of the signals approximately in the middle of the sequence which resulted in low error in this range, comparable with the error at the start and at the end of the sequence, where the force was stable. As can be seen from the three excerpts of the sequence, the signals are in alignment at the middle point (at around 50,000 samples), but they are slightly misaligned at the start (at around 10,000 samples) and at the end of oscillation (at around 90,000 samples). In this case, the signal MTM seems to have a lower clock rate than the signal REF – while the MTM signal is leading in the first part of the sequence it is lagging in the last part of the sequence. This results in the linear error increase due to signal misalignment linearly increasing with departure from the synchronized point.

In the presented case there was a significant difference in the clock rate between data from both acquisition systems and required a time scaling correction before the cross-correlation calculation for best results. With the traditional evaluation of minimum–maximum values of the cycles, this clock rate deviation, while present, is not critical. When comparing minimum–maximum values, the evaluation is based on the cycle sequence, not the sample sequence, and would be equally effective also in the case of completely arbitrary time bases, as long as the cycles can be identified and their minimum and maximum values determined. This reduces the complexity of the evaluation, but the resulting output is limited only to two points per cycle – the minimum and the maximum values of the force curve, even though a much larger dataset is available. To take advantage of the available data, the signals in their whole form could have been evaluated and also the results could have been expressed for each measured sample, significantly improving the characterisation of the indication error. The drawback of analysing the whole signal interval is the increased complexity of the evaluation, requiring more advanced methods. The signal resampling, clock-rate scaling, and cross-correlation function calculation require the application of some programming to express the results. The data analysis can be performed in any programming language, such as Python, Matlab, or any other commercially available or free open-source programming software, or simply in the Visual Basic for Application module of Microsoft Excel. All data analysis presented in this paper, including resampling, time clock-rate scaling, and cross-correlation calculation were implemented in Microsoft Excel.

For a general set of measurements, several steps are necessary to be performed and programmed to bring the signals to the same time-base and align them properly. The full evaluation procedure that was performed is the following:

1. Measure and log the signals with appropriate parameters and acquisition sampling rate.
2. Crop the signals data to the area of interest to allow for faster calculation.
3. Define the sample rate for cross-correlation (required time-shift resolution).

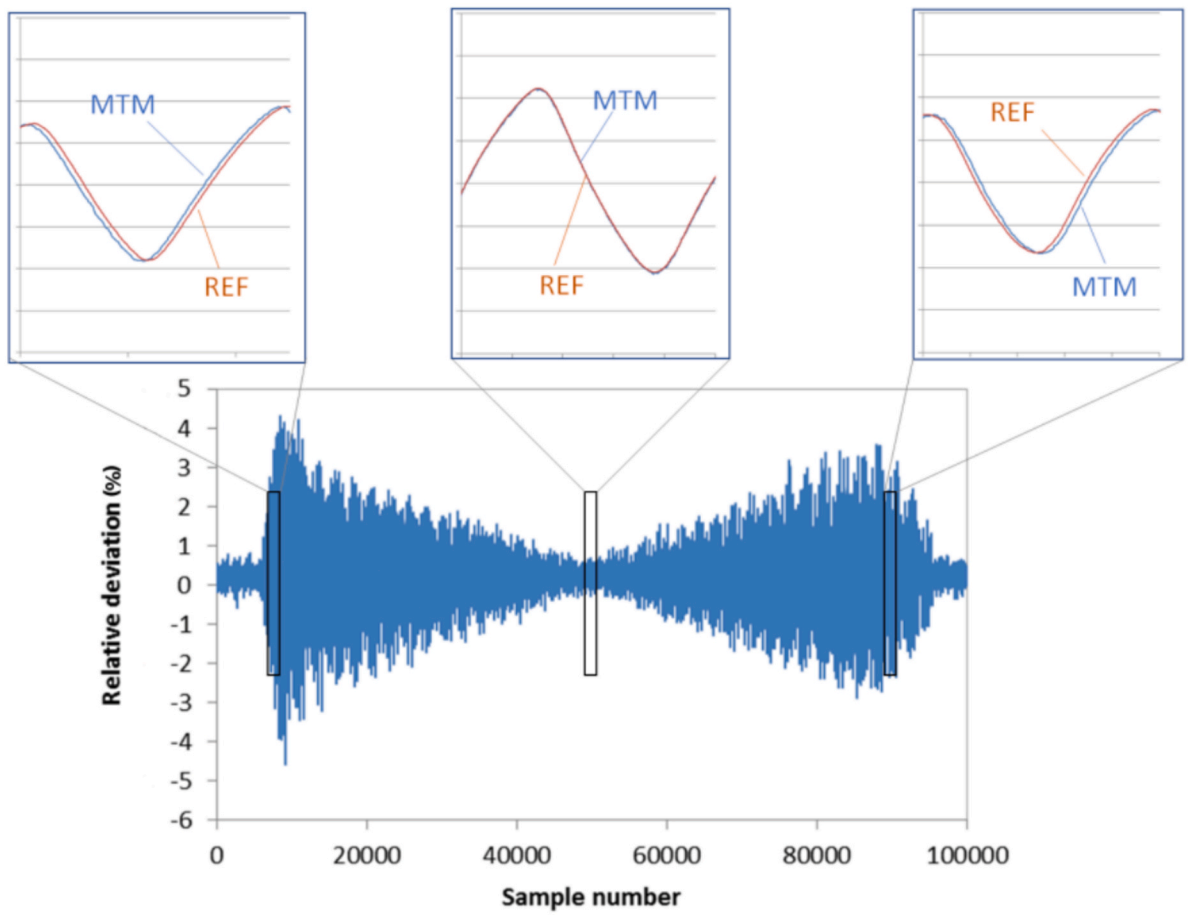


Fig. 6. Effect of the clock rate deviation of synchronized testing machine signal (MTM) and reference system signal (REF).

4. Resample the signals to the cross-correlation sample rate (either one or both if necessary, and if the cross-correlation sample rate differs from acquisition sampling rate).
5. Verify the clock rates of the signals – determine the time length of the signals between two points or over a number of cycles, and calculate the time scaling factor between the time-bases if necessary.
6. Scale the time base of one signal to match the other signal based on the scaling factor (if necessary).
7. Resample the time scaled signal to again match the sample rate interval of the second signal (if time scaling was performed).
8. Calculate the cross-correlation function and determine the necessary signal shift.
9. Align the signals according to the suggested time shift.
10. Calculate the error between the signals for the whole interval.

Not all steps are necessary in all cases, for example, if the data acquisition sampling rate is high enough and the same for both signals, there might be no need to resample any of them at first. If the clock-rate is not deviating between the signals, it might not need a correction and no scaling is necessary, and consecutively no resampling in the second pass. But in each case, the conditions need to be verified and corrected if necessary.

3. Results and discussion

The procedure for the cross-correlation function calculation was applied to the measured signals from 20 kN testing machine for 1 Hz, 5 Hz, and 10 Hz excitation from Fig. 3 and the measured signals from the

1000 kN testing machine for 1 Hz excitation from Fig. 5.

In the case of the 20 kN testing machine calibration, the testing machine force signal was sampled with 1024 samples per second while the reference force measuring system was sampled with 1200 samples per second, therefore, resampling was required for both acquired signals. In order not to change the original samples, both signals were in the first attempt upsampled to the lowest common multiple sample rate of 76800 samples per second, preserving all original measured samples and interpolated values were calculated linearly between those samples for each signal. For the measured interval of 25 s this resulted in almost two million samples for each signal. While the higher sample rate would offer better cross-correlation shift resolution, a trade-off between computational load and the time-shift resolution needs to be made. To reduce the computational load, both upsampled signals were then downsampled to 4800 samples per second. This final sample rate results in a 0.208 ms resolution of the time shift interval. Despite the sinusoidal signal, the simple linear interpolation was chosen to interpolate the values instead of a more complex interpolation function at the expense of a possibly larger error and error variation but a more general applicability also to other dynamic signal waveforms preventing interpolation overshoot. Other interpolation functions can also be used and depending on the signal sample rate, filtering settings and waveform shape could achieve better interpolation results with lower error variance but they were not investigated in this paper.

As there was about 0.025 % time scale difference between the testing machine data and the reference system data, all signal pairs were then time scaled, to assure the same actual signal time length for both signals. As the delay between the signals was in the range of about 2 s for all three excitation frequencies, the measurements were roughly aligned to

reduce the cross-correlation calculation time and the actual cross-correlation function was calculated to determine the final optimum time shift to align the signals. The signals sequences were aligned according to the calculated cross-correlation result by moving one of the signals compared to the other for the resulting number of samples. At the end, the error between the clock-rate corrected and time-aligned signals was calculated for each sample pair for the whole signal interval.

Fig. 7 shows the resulting error for the 1 Hz, 5 Hz, and 10 Hz excitation of the force transducer. It can be seen, that the error is uniform throughout the measurement interval. The average value of the error calculated for the whole series is about 0.2 % of the measured value with a calculated standard deviation of the distribution of 0.12 % for 1 Hz excitation, 0.13 % for 5 Hz excitation and 0.15 % for 10 Hz excitation. The error result at the cyclic phase of the signal in Fig. 7(a)–(c) cannot be discerned from the beginning phase of the signal, where the force was held constant, suggesting there are no additional significant effects introduced during cycling phase. This also suggests, the error could not be reduced further by improving the signal alignment, the signal noise being the limiting factor. The error distribution was in all three cases similar, an example histogram of the error distribution for the case of 10 Hz excitation is shown in Fig. 7(d).

For all three presented cases of dynamic excitation of the force transducer with 1 Hz, 5 Hz and 10 Hz the final error results are very similar and comparable. Calculating the cross-correlation function helped to optimally align the acquired signal pairs and reduced the error stemming from the signal time misalignment due to different sampling rate, filter settings in different data acquisition systems.

The same signal alignment procedure described in steps in section 2.3 was then applied also to the measured signals of the 1000 kN testing machine calibration for 1 Hz excitation from Fig. 5. The reference calibration system data acquisition was started while the testing machine was already oscillating and logging the data, resulting in much shorter reference data acquisition time than the whole testing machine data stream. The measurements were first roughly visually aligned and the testing machine data sequence cropped to about 21 s, to reduce the cross-correlation calculation time. The cropped sequence interval

included 10 cycles before and 10 cycles after the cycling frequency change. In the case of the 1000 kN machine calibration, the lower sample rate of the testing machine data acquisition of 200 Hz could be directly upsampled to the 1200 Hz sampling rate of the reference system and it was necessary to only determine interpolated values for the testing machine signal. Linear interpolation was used also in this case for the upsampled values between the original samples. Based on the 1200 Hz sampling frequency, the resolution of the time shift interval was 0.833 ms. Also in this case a significant difference in clock rate was detected between the testing machine data and the reference system data signals, requiring the time base scaling and final signal resampling before application of the cross-correlation.

Fig. 8 shows the details of the reference calibration system signal and the testing machine signal during the calibration from Fig. 5 for the 1 Hz 1000 kN testing machine calibration, showing the signals at the beginning of the sequence, Fig. 8(a), and at the end of the sequence, Fig. 8(b). The signals were manually aligned at the beginning of the series. Fig. 8 (a) shows good agreement between the signals, but Fig. 8(b), on the other hand, shows a time delay (signal shift) at the end of the same series due to the apparent frequency mismatch. As the result of the clock rate difference, the signal from the reference calibration system (ML55B – red curve) appears to have a higher frequency than the actual excitation signal measured by the testing machine (HB1000 – blue curve). This apparent frequency mismatch leads to increasing error as shown in Fig. 9. In Fig. 9, the error calculated by the direct comparison of the two signals, shown with the blue curve, increases with time towards the end of the series, going from below ± 0.5 % at the first couple of seconds at start of the sequence to above ± 6 % in 20 s measurement interval.

To eliminate the effect of the clock-rate deviation, one of the signals had to be time scaled, to assure the same actual signal time length for both systems. Both cropped signals already had the same sample sequence length – the same number of samples in the sequence, and they also had the same apparent total time length interval, based on the set sampling frequency, but due to the clock rate deviation between the signals, they were actually not the same time length. The apparently faster signal was thus time scaled to match the time base of the slower

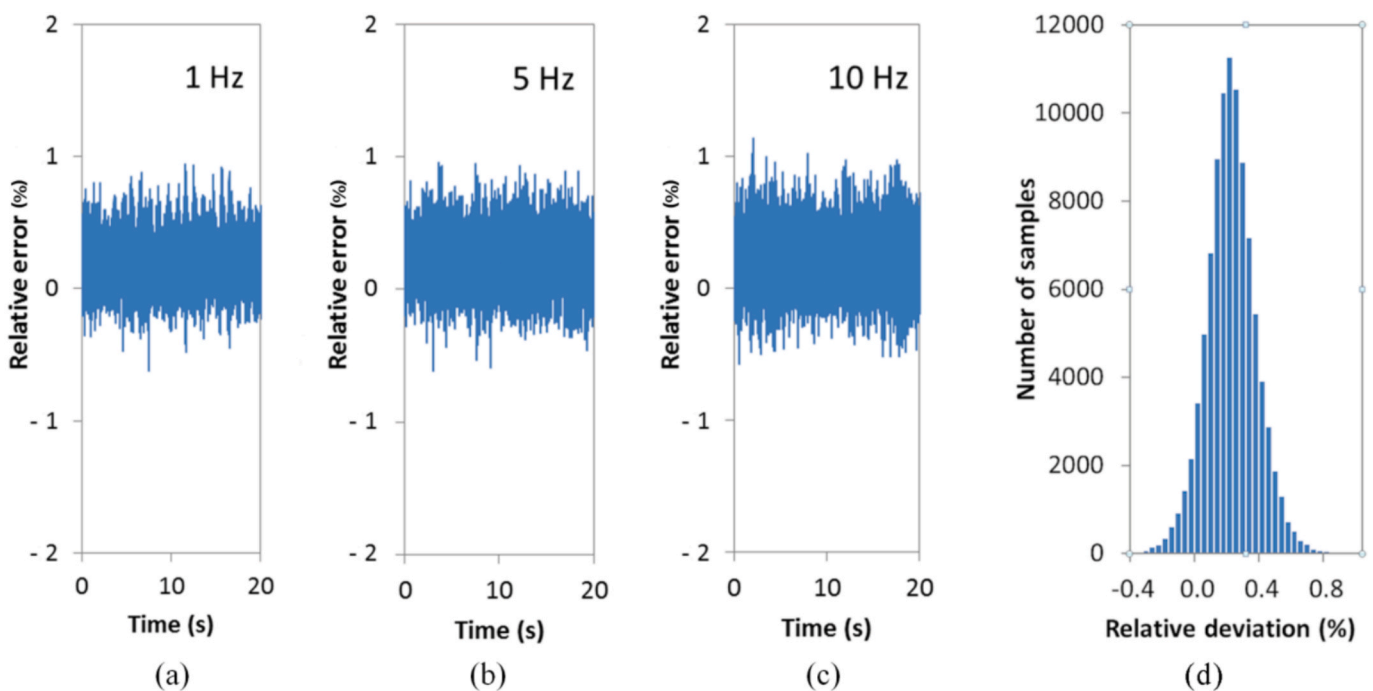


Fig. 7. Calibration errors for the 1 Hz (a), 5 Hz (b) and 10 Hz (c) cyclic excitation of the reference force transducer in the dynamic testing machine after the time misalignment correction. The standard deviation of the error distribution is 0.12 %, 0.13 % and 0.15 % respectively. The histogram of the error distribution for 10 Hz result is also shown (d).

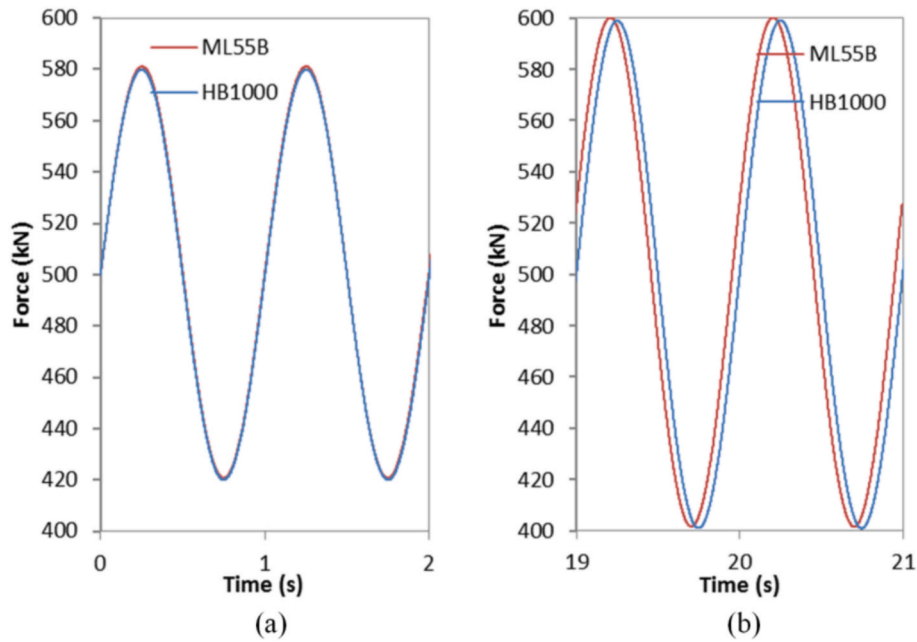


Fig. 8. Signal alignment in the case of 1000 kN testing machine calibration with 1 Hz excitation at the beginning of the series (a) and at the end of the series (b). The signals were manually aligned at the beginning of the series.

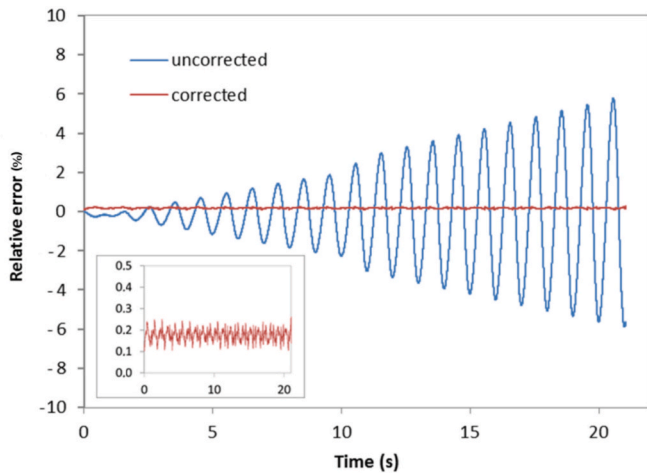


Fig. 9. Calibration errors for the 1 Hz cyclic excitation of the reference force transducer in the 1000 kN dynamic testing machine before clock rate correction (uncorrected) and after clock rate correction and cross-correlation application (corrected). The standard deviation of the final corrected signal error distribution is 0.02 % (insert) with the maximum span of ± 0.04 %.

signal. The time scaling factor was calculated from the time intervals of signal crossing the average force value (500 kN), from the first to the last crossing for the same count of cycles for each signal (maximum available cycle count). After the faster signal was time scaled to the time length of the slower signal, it was resampled to match again the sample rate of the slower signal to allow the sample by sample comparison. The actual cross-correlation function was then calculated to determine the final optimum time shift to align the sample-rate and clock-rate matched signals. Based on the result of the cross-correlation calculation result, the necessary number of samples to shift one of the signals were determined and the signals were aligned.

Finally, the error between the signals was calculated for each sample pair for the whole signal interval under investigation. The error after the clock rate correction and synchronisation based on cross-correlation function calculation is shown in Fig. 9 as the red curve (corrected).

The final error was stable within ± 0.04 % of the measured force for the whole measurement interval with standard deviation of the error sequence of 0.02 %. The signal delay synchronization and clock rate correction eliminated the error dependency on time and produced a stable error with low dispersion throughout the sequence.

The alignment of the sequence pairs was optimal for the given conditions. To verify the result, the optimally aligned sequence was shifted for one sample to the left, to decrease the delay for one sample interval, and to the right, to increase the delay for one sample interval. In this test, either increasing or decreasing the signal shift for a single sample interval produced a larger error than for the optimal alignment, as shown in Fig. 10. Shifting the signal for one sample to the left resulted in the blue curve in Fig. 10 and shifting the signal for one sample to the right resulted in the red curve in Fig. 10. Both, the blue and the red curve show increased error compared to the black curve which was the result of the optimal alignment. The error span of the optimally aligned signal increased from about ± 0.04 % to about ± 0.13 % for one-sample shifted

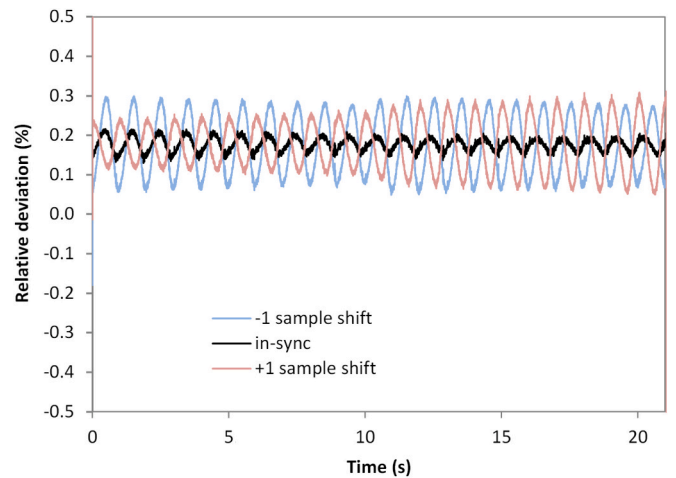


Fig. 10. Calculated error for the sequence shift for one sample to the left (blue) or one sample to the right (red) compared to the optimal synchronisation (black), 1200 Hz sampling frequency.

signals.

Also in the case of the 1000 kN testing machine calibration, the results show, that the error spread is quite uniform throughout the measurement interval. The average value of the relative error was 0.18 % of the measured values with the calculated standard deviation of the error distribution 0.02 %. The error at the amplitude change of the excitation from ± 80 kN to ± 100 kN cannot be significantly discerned from the rest of the interval. Compared to the 20 kN machine calibration error result, the much lower value of the low pass filter of the reference system for the 1000 kN testing machine calibration (100 Hz low-pass filter) versus the 1000 Hz low pass filter for the 20 kN testing machine calibration, produced significantly less noise in the signals and the noise in the resulting error standard deviation.

To investigate the effect of the sampling rate on the signal alignment and the error results, the results for the 1000 kN testing machine data were recalculated for the examples of sampling rate of 80 Hz, 200 Hz and 4800 Hz, to compare them with the 1200 Hz sampling rate results. The data from the already clock-rate corrected 1200 Hz sampling rate signals example was resampled to new sample rates and the signals were aligned optimally in the same way as in the 1200 Hz example for each new sample rate. Then the signals were shifted for one sample to the left and right for each sample rate to verify the misalignment effect. The comparison of the calculated results for 80 Hz, 200 Hz, 1200 Hz, and 4800 Hz sampling rates is shown in Fig. 11.

Fig. 11(a) shows the results for the 80 Hz sampling rate. The sampling rate of the testing machine and the reference calibration system was both resampled (downsampled) to 80 Hz. Due to the 80 Hz sampling rate, the shift interval was 12.5 ms which limited the alignment accuracy of the signals and lead to increased calculated errors. The optimally aligned signals produced larger error than the 1200 Hz sample rate example. Shifting the sequence for one sample left and right increased the error span from about ± 0.7 % of optimally aligned signals to ± 1.1 % and above ± 2 %, respectively.

Fig. 11(b) shows the results for the 200 Hz sampling rate. Here, the sampling rate of the testing machine was already acquired by 200 Hz sampling rate, and the 1200 Hz sampling rate of the reference calibration system was directly downsampled to 200 Hz, by keeping every sixth sample of the sequence and discarding the rest. Due to the 200 Hz sampling rate, the shift interval was 5 ms which again limited the alignment accuracy of the signals and lead to increased calculated errors span of ± 0.25 % compared to ± 0.04 % in the 1200 Hz example for the optimally aligned signals, but was lower than the error span of the 80 Hz sample rate example. Shifting the sequence for one sample left and right

increased the error span from about ± 0.25 % of optimally aligned signals to ± 0.4 % and ± 0.8 %, respectively.

Fig. 11(c) shows for the reference comparison the same result from Fig. 10 for 1200 Hz sampling rate. Here, due to the 1200 Hz sampling rate, the shift interval was 0.83 ms. Shifting the sequence for one sample left and right increased the error span from about ± 0.04 % of optimally aligned signals to ± 0.13 % for the shifted samples, as already shown.

Finally, Fig. 11(d) shows the results where the signals sampled with 200 Hz and 1200 Hz were upsampled to 4800 Hz. Due to the 4800 Hz sampling rate, the sample shift interval was reduced to 0.21 ms. Shifting the sequence for one sample left and right increased the error span from about ± 0.04 % of optimally aligned signals to ± 0.06 % and ± 0.05 %, respectively. The error span did not improve in this case compared to the 1200 Hz sample rate example for the optimally aligned signals, but it reduced significantly for the one-sample shifted signals, bringing them close to the level of the optimally aligned signals.

To further investigate and estimate the effect of upsampling from suggested 80 Hz sampling rate from DKD-R 9-4 guideline, the previously downsampled data from 1200 Hz to 80 Hz sample rate from Fig. 11(a) was upsampled back to 1200 Hz to compare the result with Fig. 11(c). The upsampled result (not shown) was comparable to Fig. 11(c), but the standard deviation was in this case increased slightly as the result of added noise from the linear interpolation during upsampling. The difference in errors from the original 1200 Hz sample rate results, and the same 1200 Hz signal downsampled to 80 Hz and upsampled back to 1200 Hz sample rate result was within ± 0.03 %. This error could potentially be reduced by resampling with more advanced interpolation functions instead of linear interpolation between samples or by increasing the acquisition sample rate.

In all cases presented in Fig. 11 one signal was time scaled to compensate the clock rate based on the 1200 Hz sampling frequency signals and the cross correlation function calculated to align the signals.

The results of the presented evaluations show the best estimate for the signal time shift correction between the two signals to try to achieve the smallest error variance for the given evaluation conditions. The error variance of presented results should not be taken as the final uncertainty of the force calibration result. The error variance result of the optimal time shift is only the prerequisite for the actual testing machine force calibration uncertainty calculation (according to, for example, the DKD-R 9-4 uncertainty budget for dynamic calibration) without the unwanted effects of misaligned signals. At best, the error variance can be seen as an uncertainty contribution due to the signal out-of-sync correction during dynamic force measurements. The remaining error variance or the error

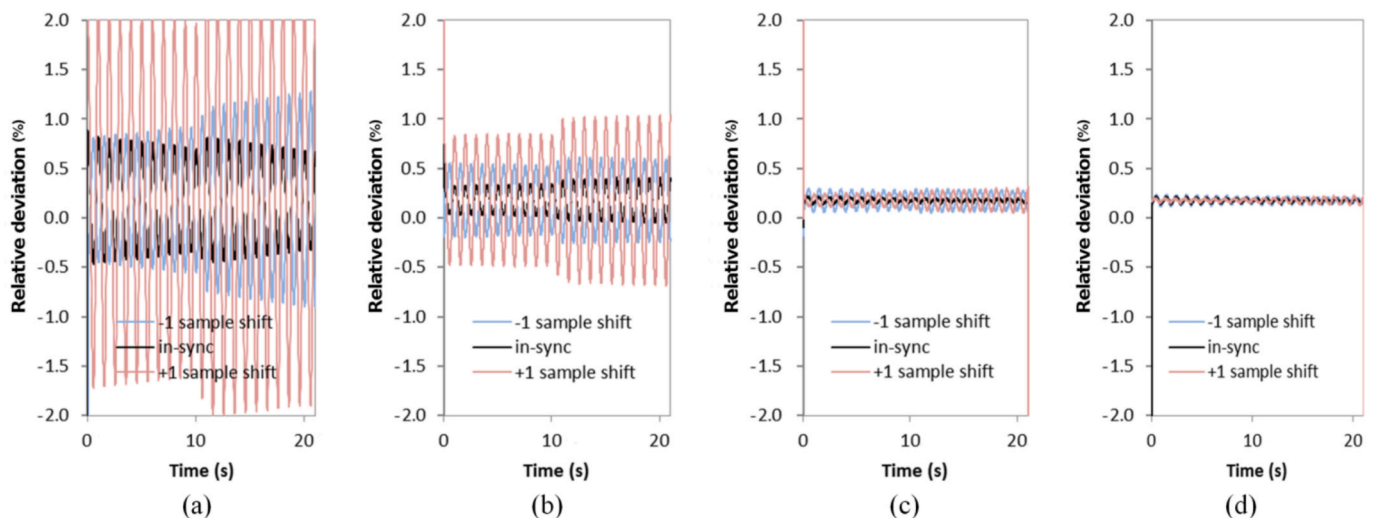


Fig. 11. Comparison of calculated errors for the sequence shift for one sample to the left (blue) or one sample to the right (red) compared to the optimal synchronisation (black), for (a) 80 Hz sampling frequency, (b) 200 Hz sampling frequency, (c) 1200 Hz sampling frequency, and (d) 4800 Hz sampling frequency.

span can be included in the uncertainty budget as it represents the remaining uncertainty effects due to signal time lag correction, namely the measurement start delay error correction, mismatched filtering delay error correction, mismatched clock-rate error correction, and the limited cross-correlation time shift resolution (sampling interval). While the errors due to filtering, clock-rate, and measurement start delay were corrected for, none of their uncertainty contributions can be individually quantified in the final result, only their sum in the form of the error variance. The cross-correlation sampling rate defines the time shift resolution which limits the final time shift correction and the final error variance even if all delay errors would be fully corrected for. The resampling interpolation error is introduced in the post-processing and it depends on the interpolation function selection, signal sampling rate before upsampling, as well as the signal frequency. This uncertainty effect is also partially included in the error variance and can also not be easily quantified individually in a universal way without additional measurements. In the most general way, the standard uncertainty due to the presented signal synchronisation procedure might be calculated from the error span limits of the resulting signal comparison as a rectangular distribution contribution (including all above uncertainty sources except the interpolation error), and the standard uncertainty due to resampling interpolation added as a separate contribution. If the maximum linear interpolation error span contribution would be, for example, as a general case estimated as the half of the force signal change within the sampled interval, calculated for the whole signal sequence in Fig. 5, it would lead to an interpolation error span of up to $\pm 0.6\%$ for upsampling the 80 Hz sampling rate signal, up to $\pm 0.3\%$ for upsampling the 200 Hz sampling rate signal, and up to $\pm 0.05\%$ for upsampling the 1200 Hz sampling rate signal. However, these values can be overestimated as in the presented case of the 1000 kN testing machine calibration, the actual interpolation error span was $\pm 0.03\%$ determined from upsampling the downsampled 80 Hz sequence back to 1200 Hz. If this interpolation error span is taken as an estimate of a rectangular distribution contribution and combined with the contribution from the signal comparison error span result of $\pm 0.04\%$ from Fig. 11(c), also as a rectangular distribution, the combined standard uncertainty of 0.03 % could be estimated as the total synchronisation uncertainty contribution.

While the proposed procedure showed promising results for signal synchronization under various data acquisition conditions regarding sample rate, filter settings and out-of-sync measurement, it has certain limitations. It is only applicable if the testing machine signal can be measured digitally and analysed, in the case of older analogue testing machines it cannot be applied. Also, very low sampling rates can significantly increase the resampling interpolation errors and might need more elaborate signal fitting functions and resampling interpolation functions. Further experiments could include more advanced interpolation functions for signal resampling to further reduce the calculated error between the signal shapes. Furthermore, the paper only investigated the case of linear time scaling, if the time error is not linear, the proposed procedure will not provide the correct results for the time error nonlinearities. With regard to clock-rate scaling, it is easier to calculate the scaling factor for periodic signals, in the case of other waveforms, additional steps will be necessary to determine correct scaling factor. The procedure focuses on finding the best agreement between the force signal shapes, but without the time calibration of the measuring systems, the time sensitive information, such as signal phase shift or exact signal timing, is lost.

4. Conclusions

The paper presented the analysis of a methodology to align the force signals acquired by different measuring systems in dynamic force testing machine calibration applications. The presented analysis of dynamic force measurement signals was based on time-misaligned signals acquired by unsynchronised measurement systems, with mismatched

sampling rates, and mismatched filter settings, with the aim to verify the possibility of signal synchronisation in post processing. The scope of investigation included testing machines of up to 1000 kN force capacity and covered tensile and compressive force loading with sinusoidal force excitation up to 10 Hz. The calibration errors were evaluated for signal sampling rates for 80 Hz, 200 Hz, 1200 Hz, and 4800 Hz.

The results show that misaligned signals with a significant time delay between them can be successfully aligned by calculating the cross-correlation function to determine the necessary time shift. Before calculating the cross-correlation function, however, signals need to be resampled to the same sampling frequency and during this process, any deviation in clock-rates must also be corrected. Completing this procedure allows the decrease of the calculated error between signals where a signal delay is the main cause for the error. This includes signal delays from unmatched low-pass filter settings, signals delays due to unsynchronised measurement start, and signals delays due to data transfer or data processing delays.

By correcting the signal clock rate and time aligning the signals, the standard deviation of the error between the testing machine indication and the reference force measuring system was reduced to well under the 1 % requirement of most standard material testing methods with standard deviation of the error below 0.2 % for all measured series, for the sinusoidal cyclic force from 1 Hz to 10 Hz in the 20 kN compression testing machine, as well as in the case of the 1000 kN tensile testing machine with 1 Hz sinusoidal excitation.

The procedure enables the characterisation of the whole measured sequence including transient effects, not only parts of the signals. The presented procedure is useful for the calibration of dynamic force measuring systems, where the force is time dependent and the measurements are typically acquired by different measuring systems introducing various time lag effects. The signal errors can be calculated for the whole signal interval instead of only for some characteristic signal points, such as peak-to-peak or min-max values.

CRedit authorship contribution statement

Miha Hiti: Writing – review & editing, Writing – original draft, Visualization, Validation, Supervision, Software, Resources, Project administration, Methodology, Investigation, Funding acquisition, Formal analysis, Data curation, Conceptualization.

Declaration of competing interest

The author declare that they have no known competing financial interests or personal relationships that could have appeared to influence the work reported in this paper.

Acknowledgments

This work is a part of the project 18SIB08 “ComTraForce” which has received funding from the EMPIR programme co-financed by the Participating States and from the European Union’s Horizon 2020 research and innovation programme.

The author acknowledges the financial support from the Slovenian Research Agency (research core funding No. P2- 0273).

Data availability

Data will be made available on request.

References

- [1] Iso, *Metallic materials—calibration of force-proving instruments used for the verification of uniaxial testing machines*, ISO 376 (2011).
- [2] Iso, *Metallic materials—calibration and verification of static uniaxial testing machines—part 1: tension/compression testing machines—calibration and verification of the force-measuring system*, ISO 7500-1 (2018).

- [3] M. Hiti, Analysis of loading profile effect on testing machine calibration results, *Meas.: Sens.* 18 (2021), <https://doi.org/10.1016/j.measen.2021.100131>.
- [4] J. Sander, R. Kumme, Comparison of force measuring devices with static and continuous loading, *Meas.: Sens.* 18 (2021), <https://doi.org/10.1016/j.measen.2021.100241>.
- [5] A. Prato, A. Improta, M. Di Lernia, S. Nobile, A. Faccelo, F. Mazzoleni, A. Germak, A. Schiavi, Static, continuous and dynamic calibration of force transducers: a comparative study on a low-force strain-gauge measuring device, *Meas.: Sens.* (2024), <https://doi.org/10.1016/j.measen.2024.101337>.
- [6] A.J. Knott, R.S. Oliveira, Effects of force application rate on transducer performance, IMEKO 24th TC3, 14th TC5, 6th TC16 and 5th TC22 International Conference, Cavtat-Dubrovnik, Croatia (2022), <https://doi.org/10.21014/tc3-2022.020>.
- [7] M. Hiti, Comparison of two 1 kN force transducers at continuous calibration, in: IMEKO 24th TC3, 14th TC5, 6th TC16 and 5th TC22 International Conference, Cavtat-Dubrovnik, Croatia, 2022, <https://doi.org/10.21014/tc3-2022.053>.
- [8] M. Hiti, Compensation of synchronization error effect in testing machine calibration, *Meas.: Sens.* 18 (2021), <https://doi.org/10.1016/j.measen.2021.100132>.
- [9] EMPIR ComTraForce Project “Comprehensive traceability for force metrology services”; Joint Research Project within the European Metrology Research Programme EMPIR 18SIB08 ComTraForce.
- [10] DKD-R 9-4: 2023, Dynamische Kalibrierung von Werkstoffprüfmaschinen : Richtlinie DKD-R 9-4, PTB, 2023.
- [11] Iso, *Metallic materials—dynamic force calibration for uniaxial fatigue testing - part 1: testing systems*, ISO 4965-1 (2012).
- [12] M. Hiti, Force signals time alignment using cross-correlation, *Meas.: Sens.* (2024), <https://doi.org/10.1016/j.measen.2024.101375>.
- [13] J. Sander, R.S. Oliveira, F.L. Tegtmeier, A. Knott, Optimised data synchronisation methods for continuous force calibration, *Meas.: Sens.* (2024), <https://doi.org/10.1016/j.measen.2024.101341>.
- [14] T. Dare, Synchronization in multi-sensor measurements: importance and methods. Internoise 2022 - 51st International Congress and Exposition on Noise Control Engineering, Glasgow, United Kingdom, 2022.
- [15] J.C. Santamarina, D. Fratta, *Discrete Signals and Inverse Problems: an Introduction for Engineers and scientists*, John Wiley & Sons, 2005.
- [16] R. Quian Quiroga, A. Kraskov, T. Kreuz, P. Grassberger, Performance of different synchronization measures in real data: a case study on electroencephalographic signals, *Phys. Rev. E* 65 (2002) 041903, <https://doi.org/10.1103/PhysRevE.65.041903>.